

What's in the Black Box?

The False Negative Mechanisms Inside Object Detectors

Dimity Miller^{1,2}, Peyman Moghadam¹, Mark Cox¹, Matt Wildie¹ and Raja Jurdak²

Abstract—In object detection, false negatives arise when a detector fails to detect a target object. To understand *why* object detectors produce false negatives, we identify five ‘false negative mechanisms’, where each mechanism describes how a specific component inside the detector architecture failed. Focusing on two-stage and one-stage anchor-box object detector architectures, we introduce a framework for quantifying these false negative mechanisms. Using this framework, we investigate why Faster R-CNN and RetinaNet fail to detect objects in benchmark vision datasets and robotics datasets. We show that a detector’s false negative mechanisms differ significantly between computer vision benchmark datasets and robotics deployment scenarios. This has implications for the translation of object detectors developed for benchmark datasets to robotics applications.

I. INTRODUCTION

Given an image, object detectors identify target objects in terms of *where* they are and *what* they are. Detectors are useful tools for a range of robotics tasks – from object-centric mapping [1], to search-and-rescue missions [2], pest control in protected environments [3], and automated harvesting [4]. In each of these applications, the detector is one of the first components in a complex system, and its predictions can dictate the decisions made by follow-on components. As such, the detector has the potential to influence the performance of the entire system.

Within the computer vision community, regular advances have produced object detectors that perform increasingly well on benchmark datasets such as COCO [5]. Yet when deployed on real-world challenging conditions – poor lighting [6], varying viewpoints [6], object occlusions [7], and unknown objects [8], [9] – otherwise high-performing detectors have been shown to deteriorate, exhibiting an increase in false object predictions, or failing to detect objects altogether. A recent real-world example of this was the DARPA Subterranean (SubT) Challenge [10], where a team of autonomous robots were required to detect and localise target objects (*e.g.* survivors) in a subterranean environment. The subterranean environment posed major challenges for object detectors, with poor lighting, airborne dust, and unusual object viewpoints. This performance drop in challenging environments, alongside an inability to express predictive uncertainty, raises

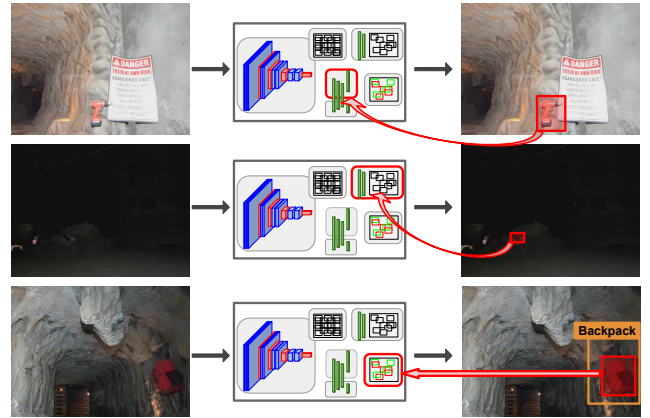


Fig. 1: We look inside an object detector to identify which component of the architecture failed to detect an object. In the top image, the classifier confuses the object with the background. In the middle image, the detector’s Region Proposal Network doesn’t propose a region for the object. In the bottom image, the poorly localised detection suppressed a correctly localised detection. Images are from Team CSIRO Data61 in the DARPA Subterranean Challenge (SubT).

genuine questions about the reliability of object detectors for robotic systems [11].

In this paper, we examine the phenomenon of false negative failures in object detection. False negatives occur when a detector does not detect an object that is present – either by silently failing to detect the object’s presence entirely, or by miscalculating the object’s location or classification, preventing association with the ground-truth object during evaluation. We show an example of both in Figure 1. Previous works examining false negatives describe these errors by examining the output of an object detector, treating the detector itself as a black box [12]. While this provides a descriptive categorisation of detection errors, it does not establish *why* object detectors produce false negatives. Seeking to answer this question, we instead examine *inside* the architecture of object detectors, identifying the specific component of the detector architecture that failed. By taking this alternate approach, we hope to inform future research into how to mitigate false negative errors and improve the reliability of detectors for robotic systems.

Focusing on two-stage and one-stage anchor-box object detector architectures [13]–[18], this paper proposes to distinguish five false negative mechanisms and introduces a framework for their identification. Using this framework, we

¹ Authors are with the Robotics and Autonomous Systems, DATA61, CSIRO, Brisbane, QLD 4069, Australia.

² Authors are with the Trusted Networks Lab at the Queensland University of Technology (QUT), Brisbane, Australia.

Dimity Miller acknowledges continued support from the CSIRO’s Machine Learning and Artificial Intelligence Future Science Platform (MLAI FSP). Contact: d24.miller@qut.edu.au

investigate different detectors' false negative mechanisms on a combination of benchmark computer vision and robotics datasets that contain challenging conditions. With this approach, we show that the false negative mechanisms of a detector on benchmark datasets do not reliably indicate why a detector will fail in robotics applications with different conditions. In addition, we show that false negative mechanisms from a detector are highly dependent on context-dependent challenging conditions.

II. BACKGROUND

Object detection is the task of identifying a set of 'target' objects in an image. This requires the specification of a set of object categories, where objects of this type are of interest and should be detected, and everything else is considered as part of the 'background' of an image and should not be detected. For example, if 'person' and 'dog' are the only target objects, then trees, fences, frisbees, and everything else, belong to the background category.

Each image contains a set of ground-truth, target objects. Each ground-truth object is described by a bounding box that tightly fits the object, and a class label describing the object category. An object detector identifies these target objects with a set of detections. Each detection contains a predicted object bounding box, a predicted class label, and a score for the detector's confidence in the predicted classification. A perfectly performing object detector has a detection that exactly matches every object, and no extraneous detections.

On a dataset of images, the primary metric used to summarise object detection performance is mean Average Precision (mAP) [5], [19]. mAP is the mean of the Average Precision (AP) for each target object class, where AP is the area under a precision-recall curve. The precision-recall curves calculates the number of 'true positive' detections, 'false positive' detections, and 'false negative' objects for each target class. A detection is a true positive if it localises and correctly classifies an object that has not already been detected by a previous detection. Localisation is measured by the Intersection-over-Union (IoU) between the object bounding box and the detection predicted box, and must be greater than a specified threshold – typically an IoU of at least 0.5 is required [5], [19]. If the detection does not meet this threshold with any undetected objects of its predicted class, it is a false positive. A false negative describes an object that was not associated with a detection during the evaluation – *i.e.* there were no detections with the correct class label and an IoU greater than 0.5.

III. PRIOR WORK

As established in Section II, the primary metric assessing object detection performance is mAP. With the mAP metric, failures in object detection can only be coarsely described as false positives or false negatives. To further understand *why* a detection is considered a failure, Hoiem *et al.* [20] introduced a categorisation for false positive detections.

More recently, Bolya *et al.* [12] built upon this categorisation to include categories describing false negative objects,

also improving the generalisability of the categorisation to different datasets. Their work introduces TIDE, which describes six categories for failures in object detectors:

- 1) Classification (Cls) errors: a detection localises an object of the incorrect object class.
- 2) Localisation (Loc) errors: a detection overlaps an object of the correct class, but with poor localisation.
- 3) Both Classification and Localisation (Cls+Loc) errors: a detection overlaps an object of the incorrect object class, but with poor localisation.
- 4) Duplicate errors: a detection localises an object of the correct object class, but that object has already been associated with a higher scoring detection.
- 5) Background errors: a detection does not overlap with an object from any target object class.
- 6) Missed GT errors: any undetected ground-truth object that is not due to a Cls, Loc or Cls+Loc error.

These failure categories can represent both false positives and false negatives – in fact, a false negative failure can be a Cls, Loc, Cls+Loc, or Missed GT error.

TIDE [12] categorises false negatives by asking the question – why didn't the predicted detections capture the false negative object? This places the emphasis on the output of the detector, and treats the detector as a black box. In contrast, our work asks the question – why didn't the detector produce a detection that captured the false negative object? With this distinction, we focus on the detection process occurring *inside* the object detector, and can identify the specific component of the detector that failed and led to the false negative outcome. We refer to these as false negative mechanisms of an object detector.

As we will show in Section VI, while TIDE provides descriptive terminology for categorising the output of a detector as failures, it does not provide an intuitive understanding of the corresponding false negative mechanism. For example, a natural assumption would be that localisation errors are caused by failures in the localisation component of the object detector. This is an *incorrect assumption*. Instead, TIDE localisation errors primarily correspond to failures in the classification component of the detector (*e.g.* see Figure 4). For the purpose of understanding why detectors produce false negatives, our categorisation instead directly highlights the detector component that failed and how.

In the last few years, a number of works have emerged introducing techniques that identify when an object detector fails to detect an object [21]–[23]. These works all highlighted the danger of false negatives in object detectors aboard autonomous systems, arguing potentially catastrophic consequences in applications such as autonomous driving [21]–[23]. Without any existing research informing why object detectors produce false negatives, these works instead focused on exploiting other signals for detecting false negatives – temporal or stereo camera detection inconsistencies [22], learning underlying biases in the objects that produce false negatives [23], and relying on hand-crafted indicators of false negatives in a detector's feature maps [21].

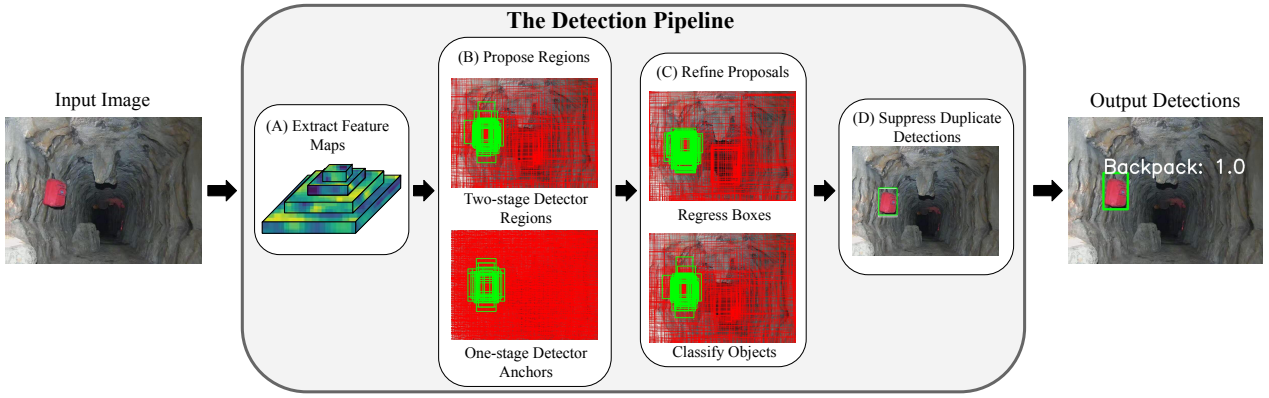


Fig. 2: We identify a ‘detection pipeline’ within object detectors that facilitates correct detections of objects. A failure at any step in the pipeline can prevent an object from being detected, and create a false negative. At each step, correct predictions are shown with the green, thick-lined boxes – i.e. boxes that correctly localise or correctly classify the object.

IV. OUR PROPOSED FRAMEWORK

Our approach for establishing why detectors fail is grounded in understanding how a detector functions to correctly detect an object. Figure 2 visualises a four step ‘detection pipeline’ that is used for most two-stage and one-stage anchor-box detector architectures, where each step plays an important role in detecting an object, and thus also has the potential to fail and cause a false negative failure.

In this section, we detail each step in the detection pipeline, focusing on the role of different components of the architecture as observed from existing two-stage and one-stage anchor-box detectors, including Faster R-CNN [13], Cascade R-CNN [15], SSD [18], YOLOv2 [16], YOLOv3 [17], and RetinaNet [14]. At each step, we then introduce a false negative mechanism and how it can be identified. Finally, we present this framework as an algorithm that can be used to identify false negative mechanisms in two-stage and one-stage anchor-box object detectors.

A. Extracting Features from an Image

Before an object can be localised or classified, semantic information and visual features need to be extracted from image pixels. In object detectors, this is performed by convolutional ‘backbones’, which are typically re-purposed from high-performing image classifiers [13]–[18]. Most modern detectors combine a convolutional backbone with a Feature Pyramid Network (FPN) [14], [15], which is able to detect objects of various sizes by producing a set of semantically-rich, scaled feature maps [24].

Feature backbones are ubiquitously initialised with parameters from pre-trained classifiers that perform highly on image recognition tasks [13]–[18], and are accepted as extracting general image features. While the performance of the feature backbone influences down-stream components in the detector architecture, it does not localise or classify objects itself, and thus we do not identify it as a mechanism for false negatives.

B. Proposing Potential Object Regions

Given the feature maps extracted in the previous step, the detector identifies image regions that may contain objects. This is handled differently between two-stage and one-stage anchor-box architectures.

Two-stage architectures rely on fully convolutional networks, known as Region Proposal Networks (RPN) [13], [15], to propose a set of image regions that may contain an object. In this step, two-stage detectors define a dense grid of ‘anchors’ over the computed feature maps. Each anchor represents a bounding box with a different centre point, scale, and aspect ratio. The RPN is then applied to each anchor, predicting ‘objectness’ scores and regressing the anchor boundaries to tightly fit any present object. The anchors with the top-k highest objectness scores, and their regressed bounding boxes, are then output from the RPN as the initial set of object proposals.

Similar to two-stage detectors, one-stage anchor-box architectures segment feature maps into a grid of anchor boxes [14], [16]–[18]. However, rather than using an RPN to filter these anchor boxes into region proposals, they instead treat *every* anchor box as a region proposal. This creates a much greater number of object proposals, and instead relies on later steps in the pipeline to filter out the anchors that do not contain an object.

Proposal Process False Negative Mechanism: In this step, we identify that a false negative can be produced if no object proposals localise a given target object. We refer to this as a ‘proposal process’ false negative mechanism. Without a proposal for the object’s image region, later steps in the detection pipeline will not be input the features necessary to accurately classify or localise the object. We identify this mechanism by computing the IoU between the target object bounding box and all object proposals, where an IoU of at least θ_{loc} is required for an object to be considered localised.

In a two-stage architecture, the proposal process false negative mechanism may occur for two reasons: (1) none of the RPN regressed anchors sufficiently localised the object,

or (2) the anchors that did localise the object were assigned low objectness scores by the RPN.

In a one-stage anchor-box architecture, the proposal process false negative mechanism occurs if no anchor boxes localise a target object. Given the grid-like, dense sampling of anchor boxes, this is far less likely to occur than in a two-stage architecture. For example, given a 640x480 image, a two-stage Faster R-CNN produces 1000 RPN object proposals [13], whereas the one-stage RetinaNet produces 163206 anchor boxes [14].

C. Refining Object Proposals

The detector then refines the large number of object proposals to determine whether they contain an object, and if so, the classification of the object and its exact location in the image. For both two-stage and one-stage anchor-box detectors, this is typically achieved with two components: (1) a bounding box regressor, and (2) an object classifier.

1) *Bounding Box Regressor*: To localise the object, regions of interest are extracted from the feature maps for each object proposal bounding box and passed into the bounding box regressor. The bounding box regressor is typically a small Fully Convolutional Network [13]–[18], and predicts changes, or offsets, to the initially proposed bounding box from the prior step. Often detectors utilise multiple bounding box regressors, with different regressors operating on different feature maps [13], [14], [16]–[18], or being used for iterative bounding box refinement [15].

Regressor False Negative Mechanism: Assuming an object proposal localises an object, the regressor should predict offsets that improve this localisation. However, the regressor may produce offsets that reduce the overlap of the bounding box with a target object. We refer to this as a ‘regressor’ false negative mechanism. We identify this mechanism when there are no regressed bounding boxes with an IoU of at least θ_{loc} with the target object box, despite the presence of a proposal box that had localised the object.

2) *Object Classifier*: Similar to the regressor, the object classifier is typically a small Fully Convolutional Network that intakes the features of each object proposal [13]–[18]. Again, detectors frequently utilise multiple object classifiers to operate on different feature maps [13], [14], [16]–[18]. In some architectures, the classifier shares layers with the regressor [13], [15]–[18], whereas in others it is an entirely separate network [14]. The classifier must determine which class an object proposal belongs to – distinguishing between the different target object classes and the background class. For every object proposal, the classifier outputs a confidence score for each target class and the background class, where high confidence scores indicate the class the proposal belongs to. The YOLO-series detectors [16], [17] also predict an ‘objectness’ score that represents the likelihood a proposal contains an object. The objectness score is multiplied with the class confidence scores to create an objectness-aware class confidence score. For all detectors, a minimum confidence score is specified as a parameter of the detector, θ_{cls} . All proposals with a target class score above this

minimum score threshold form a detection, which contains the target class label, associated confidence score, and the refined bounding box from the regressor.

While a proposal may have localised an object, the classifier can produce a false negative if it does not assign a classification score above θ_{cls} to the correct target object class. This can happen for two different reasons, and thus we identify two possible classification false negative mechanisms at this step.

Interclass Classification False Negative Mechanism: In some cases, the classifier can confuse an object for another incorrect target class. We refer to this as an ‘interclass classification’ false negative mechanism. Given the classification scores of boxes that have localised the target object, we identify this mechanism when the classifier assigned any incorrect target classes a confidence score above θ_{cls} .

Background Classification False Negative Mechanism: The classifier can also fail by misclassifying all proposals of the object as belonging to the background of the image, i.e. the ‘background’ class. Assuming an interclass classification mechanism has not been identified, we identify this ‘background classification’ mechanism when all localised boxes of the object are assigned a background class confidence score above θ_{cls} .

D. Suppressing Duplicate Detections

Given the large number of object proposals from Step B, even after refining the detections, there is often multiple overlapping detections that jointly detect a single object with the same predicted class label. Non-Maximum Suppression (NMS) is an algorithm commonly used by object detectors to suppress duplicate detections of a single object [13]–[18]. For each target class, it ranks all predicted detections from the highest class confidence score to the lowest. Moving from top to bottom, any detection that highly overlaps with a more confident detection is suppressed. Typically, an overlap threshold of IoU greater than 0.5 is used. Any detections remaining are finally output as object predictions from the object detector.

Classifier Calibration False Negative Mechanism: NMS relies on the best localised bounding boxes having the highest classification confidence scores. If this assumption is not satisfied, a false negative can be introduced when a correctly localised detection is suppressed by a detection that has not localised the object, *i.e.* IoU less than θ_{loc} . We refer to this as a ‘classifier calibration’ false negative mechanism, as it is ultimately the fault of the calibration of the classifier’s confidence scores – detections that better localise an object should be coupled with higher confidence scores from the classifier. Prior to NMS, we can identify this false negative mechanism when there is a regressed bounding box that localises the target object with an IoU greater than θ_{loc} (correctly localised), that also has a confidence score for the correct target class above θ_{cls} (correctly classified), but it is not produced as an output detection.

Algorithm 1 Identifying the Mechanism of a False Negative in Object Detection

Notation:

$$\begin{aligned}
 b, c & \\
 N, N + 1 & \\
 \hat{P} = \{\hat{p}_1, \dots, \hat{p}_k\} & \\
 \hat{B} = \{\hat{b}_1, \dots, \hat{b}_k\} & \\
 \hat{S} = \{\hat{S}_1, \dots, \hat{S}_k\}, & \\
 \text{where } \hat{S}_i = [s_{i,1}, \dots, s_{i,N}, s_{i,N+1}] & \\
 \theta_{loc}, \theta_{cls} &
 \end{aligned}$$

▷ the bounding box and class label index of the false negative object
 ▷ the number of target object classes and the index of the background class
 ▷ a set of k proposal bounding boxes produced in Step B of the detection pipeline
 ▷ a set of k bounding boxes refined by the regressor in Step C of the detection pipeline
 ▷ a set of classification score lists from Step C in the detection pipeline
 ▷ a list of confidence scores for each target class and the background class
 ▷ IoU threshold for object localisation and score threshold for object classification

Compute:

$$\begin{aligned}
 IoU_{\hat{B}} &= IoU(b, \hat{B}) \\
 \text{if any } IoU_{\hat{B}} \geq \theta_{loc} \text{ then} & \\
 S_{localised} &= \mathbf{S}[IoU_{\hat{B}} \geq \theta_{loc}] \\
 \text{if any } S_{localised}[c] \geq \theta_{cls} \text{ then} & \\
 \text{return "Classifier Calibration"} & \\
 \text{else if any } S_{localised}[1:N] \geq \theta_{cls} \text{ then} & \\
 \text{return "Interclass Classification"} & \\
 \text{else} & \\
 \text{return "Background Classification"} & \\
 \text{else} & \\
 IoU_{\hat{P}} &= IoU(b, \hat{P}) \\
 \text{if any } IoU_{\hat{P}} \geq \theta_{loc} \text{ then} & \\
 \text{return "Regressor"} & \\
 \text{else} & \\
 \text{return "Proposal Process"} &
 \end{aligned}$$

▷ IoU between all regressor-refined boxes and the false negative box
 ▷ Object was localised by a regressed box
 ▷ The set of classification score lists for the localised boxes
 ▷ A localised box had also correctly classified the target object
 ▷ A correct detection was suppressed in Step D of the pipeline
 ▷ A localised box confused the object for a different target class
 ▷ A localised box confused the object for the background class
 ▷ The object was not localised by any regressed boxes
 ▷ IoU between all object proposal boxes and the false negative box
 ▷ Object was localised by an object proposal
 ▷ The regressor incorrectly regressed from the object proposal box
 ▷ No object proposals localised the object

E. An Algorithm For Identifying False Negative Mechanisms

Given our five identified false negative mechanisms – proposal process, regressor, background classification, interclass classification, and classifier calibration – we formalise their identification for any given false negative in Algorithm 1.

V. EXPERIMENTAL SETUP

In this section, we detail the object detectors, datasets, and implementation details used to investigate our framework for identifying false negative mechanisms.

A. Object Detectors

We evaluate with two object detectors: Faster R-CNN [13], and RetinaNet [14]. Faster R-CNN is the classic two-stage object detector, and despite being developed nearly 7 years ago, it maintains competitive performance on the COCO benchmark challenge when combined with state-of-the-art feature backbones [25]. RetinaNet is a popular one-stage anchor-box object detector, and the first of its kind to obtain competitive performance with two-stage detectors [14].

B. Datasets

We evaluate across a combination of benchmark computer vision and robot-collected datasets:

The **COCO dataset** [5] is the predominant benchmark dataset for evaluating object detectors. We evaluate with the ‘val2017’ split of the dataset, which contains 4952 images featuring objects from 80 different target classes.

The **Exclusively Dark (ExDark) dataset** [26] is a public dataset containing 7363 images from low-light indoor and outdoor environments. Target object classes include bicycle, boat, bottle, bus, car, cat, chair, cup, dog, motorbike, person, and table. While challenging illumination is relevant

to robotics applications, ExDark was collated with images sampled from internet websites rather than robot-collected. The **iCubWorld Transformation (iCubWorldT) dataset** [27] is a public dataset collected by an iCub humanoid robot [28]. Images were collected with a human randomly rotating an object before the robot. As a result, the dataset features objects from a variety of challenging viewpoints. We test on 2400 images that contained target object classes overlapping with COCO, specifically images of books, bottles, and cups. The **CSIRO Data61 Subterranean Robot dataset** consists of 5384 images collected by Team CSIRO Data61 [29] during the final event of the DARPA Subterranean (SubT) Challenge [10]. During this event, a robot fleet was required to explore an unknown subterranean environment under the supervision of a single human operator, and detect and localise a set of target objects – namely survivor, backpack, fire extinguisher, helmet, rope, cell phone, colored cube, drill, and air-vent. The test images in this dataset are from the RGB cameras aboard Team CSIRO Data61’s robot fleet, and were collated by extracting frames with tracked artefacts from the team’s 3D tracking and artefact visibility system. For each extracted frame, we hand-labelled annotations for any present objects.

C. Implementation

For both detectors, we use the public implementation available via detectron2 [25] and a ResNet50 [30] with Feature Pyramid Network [24] backbone. For experiments on the COCO, ExDark and iCubWorldT datasets, the detectors are trained with the ‘train’ subset of the COCO dataset [5]. For experiments on the CSIRO Data61 SubT dataset, we train both detectors with the training dataset used by Team

TABLE I: False negative rates on each dataset.

	# Objects	False Negative Rate (#)	
		Faster R-CNN	RetinaNet
COCO [5]	36335	30% (10903)	32.7% (11872)
iCubWorld [27]	2400	37.5% (901)	48.5% (1165)
ExDark [26]	23710	28.5% (6749)	30.3% (7181)
CSIRO Data61 SubT	5428	17.2% (936)	16.5% (895)

CSIRO Data61, which consists of approximately 28,000 images collected in-house.

When implementing the framework for identifying false negative mechanisms, we use the standard localisation threshold θ_{loc} of 0.5 [5], [19], and a classification score threshold θ_{cls} of 0.3. A public implementation of our framework will be made available upon acceptance for publication.

VI. RESULTS

A. False Negative Mechanisms versus False Negative Error Types

As shown in Table I, Faster R-CNN and RetinaNet fail to detect 30% and 32.7% of all target objects in the COCO dataset [5]. In Figure 3, from left to right, we compare the distribution of our identified false negative mechanisms, the distribution of TIDE’s false negative error types [12], and the relationship between our false negative mechanisms and the TIDE error types. First examining our identified false negative mechanisms, two key insights are clear across both detector architectures:

- 1) The classifier causes most false negatives – between 77.5% (Faster R-CNN) to 94% (RetinaNet) of all false negatives.
- 2) The regressor rarely fails to localise an object – between 0.1% (RetinaNet) to 2.5% (Faster R-CNN) of all false negatives.

The Background Classification false negative mechanism is the primary mechanism of failure, where a bounding box that localised the object existed, but was misclassified as belonging to the background class. Class imbalance between foreground and background of the image is one of the well-established challenges in the object detection task [31], and thus this result is consistent with existing literature.

RetinaNet particularly struggles with this foreground-background imbalance, with 19.7% more Background Classification mechanisms than Faster R-CNN. Instead, Faster R-CNN exhibits an increase in Proposal Process false negatives, with 14.1% more of this mechanism than RetinaNet. These differences in false negative mechanisms are again consistent with the expected challenges of each architecture – Faster R-CNN first filters out anchor boxes of the image background with its Region Proposal Network, and then again with the classifier when proposals are refined [13]. In contrast, RetinaNet does not filter its anchor boxes during the proposal process, instead relying solely on the classification component of the architecture to filter out the large number of background proposals [14].

Examining the false negative error types introduced by the TIDE categorisation [12], the majority of false negatives belong to the ‘Missed’ category – between 47.2% (Faster R-CNN) and 51.9% (RetinaNet). The remaining false negatives mostly belong to a ‘Localisation’ error category (Localisation alone, or Localisation and Classification) – 39.5% (RetinaNet) to 41.6% (Faster R-CNN).

The right side of Figure 3 shows the composition of our identified false negative mechanisms for each of the TIDE error types. We observe that most of the TIDE error types can be produced by multiple different false negative mechanisms. For example, as shown in Figure 4, while the ‘Missed’ errors appear identical from the output of the detector, looking inside the detector can reveal either a Proposal Process or Background Classification false negative negative mechanism. Additionally, TIDE error types do not always intuitively signal the false negative mechanism. For example, while the ‘Localisation’ error type suggests a failure in the localisation component of an object detector, the majority of these false negatives are caused by classifier mechanisms. An example of this is visualised in Figure 4, where the ‘Localisation’ error was caused by a ‘Classifier Calibration’ false negative mechanism – a correctly localised detection existed, but it was suppressed as it had a lower confidence score. These results indicate that our false negative mechanisms, rather than the TIDE [12] error types, yield more transparent and intuitive insights into why detectors produce false negatives.

B. False Negative Mechanisms in Challenging Conditions

Table I and Figure 5 show respectively the false negative rate and distribution of our identified false negative mechanisms on the datasets with challenging perception conditions. We observe three key insights from these results:

- 1) The distribution of false negative mechanisms is fairly consistent amongst the internet-collected, benchmark datasets COCO and ExDark – yet this distribution does not reliably indicate the false negative mechanisms present on the robot-collected datasets iCubWorldT and CSIRO Data61 SubT.
- 2) Among the robot-collected datasets, discrepant false negative mechanisms are observed. For iCubWorldT, the predominant mechanism is Interclass Classification, whereas for CSIRO Data61 SubT, the predominant mechanism is Background Classification.
- 3) Despite the differences across the datasets, the distribution of false negative mechanisms is consistent across the two different detector architectures.

The iCubWorldT dataset, featuring challenging viewpoints of objects in indoor environments, primarily produces false negatives through the Interclass Classification mechanism – an increase of 44.2% (Faster R-CNN) and 54.6% (RetinaNet) compared to COCO. This indicates that the primary challenge for objects in unusual viewpoints is discriminating between target object classes. We infer this is due to a lack of training images with those viewpoints, thus the detector cannot learn to discriminate at those viewpoints.

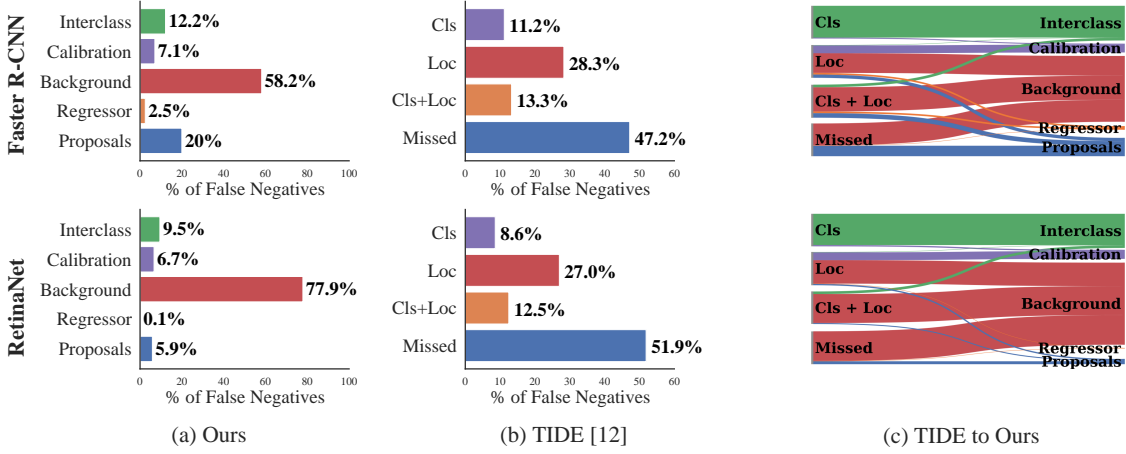


Fig. 3: We compare (a) our identified false negative mechanisms to (b) the TIDE [12] error types when detectors are tested on COCO val2017. In (c), a Sankey plot visualises the mapping from TIDE error types (left) to our identified false negative mechanisms (right), where the width of the connecting lines is proportionate to the relative composition of each error type.

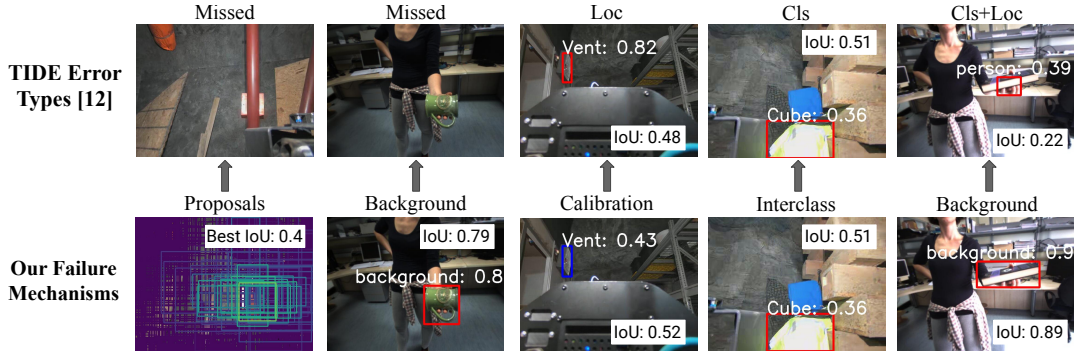


Fig. 4: For a selection of false negatives, we compare the TIDE error type [12] with our identified failure mechanism. The IoU with the target object is indicated where relevant.

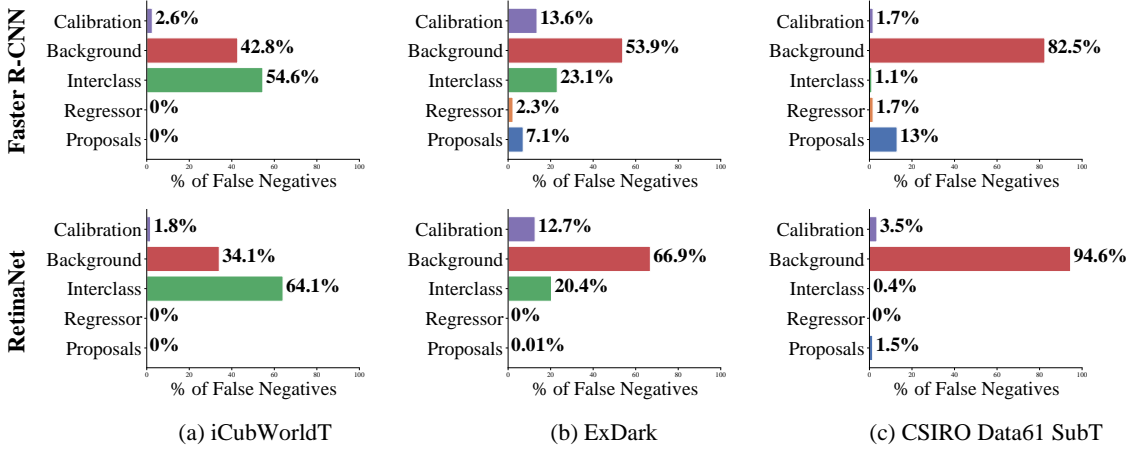


Fig. 5: The distribution of our identified false negative mechanisms on datasets containing challenging perception conditions.

For the CSIRO Data61 SubT dataset, the Background Classification mechanism dominates as the source of false negatives, responsible for 82.8% (Faster R-CNN) to 94.6% (RetinaNet) of all false negatives. All other false negative mechanisms are significantly reduced or negligible. The difference in false negative mechanisms across the standard

benchmark datasets and the robot-collected datasets has interesting implications about the transfer of research from the computer vision community to the robotics community – techniques developed to improve detectors for benchmark vision datasets may not offer the same performance improvement in a robotics application. For example, while “solving”

all non-Background false negative mechanisms would yield a 22.1% (RetinaNet) to 41.2% (Faster R-CNN) reduction in false negatives on COCO, it would only remove 5.4% (RetinaNet) to 17.5% (Faster R-CNN) of false negatives for the subterranean detection application represented by the CSIRO Data61 SubT dataset.

ExDark follows the false negative mechanism trends of the COCO dataset. While there are slight differences – less Background Classification and Proposal Process mechanisms and more Interclass Classification and Classifier Calibration mechanisms – the distributions are mostly consistent. We infer this similarity is because ExDark is composed of internet-collated images, similar to COCO, and thus is likely to contain similar biases in image structure and content.

VII. CONCLUSIONS

In this paper, we identified five mechanisms within an object detector that can cause a false negative failure. Investigating these mechanisms on computer vision and robotics datasets, we highlighted that reduced false negatives on benchmark datasets does not reliably indicate reduced false negatives on robot-collected data. Our proposed framework could be used to facilitate selection of object detectors and techniques that may best translate to robotics applications.

The overarching goal of this work is to enable future research into object detection architectures that are robust to false negatives. Yet quantifying the false negative mechanisms of an object detector also has broader implications. For example, our proposed framework could be used for targeted data collection to improve object representation in the training dataset, *e.g.* re-training with object viewpoints that lead to Interclass Classification failures. With the ability of robots to localise in their environments, this could also be adapted to an online learning scenario – after detecting an object that was undetected in a previous frame, the system could analyse which component of the detector failed, and perform targeted online learning with any collected data.

REFERENCES

- [1] L. Nicholson, M. Milford, and N. Sünderhauf, “Quadricslam: Dual quadrics from object detections as landmarks in object-oriented slam,” *IEEE Robotics and Automation Letters*, vol. 4, no. 1, pp. 1–8, 2019.
- [2] J. Sandino, F. Maire, P. Caccetta, C. Sanderson, and F. Gonzalez, “Drone-based autonomous motion planning system for outdoor environments under object detection uncertainty,” *Remote Sensing*, vol. 13, no. 21, p. 4481, 2021.
- [3] J. Liu, B. Kusy, R. Marchant, B. Do, T. Merz, J. Crosswell, A. Steven, N. Heaney, K. von Richter, L. Tychsen-Smith *et al.*, “The csiro crown-of-thorn starfish detection dataset,” *arXiv preprint arXiv:2111.14311*, 2021.
- [4] I. Sa, Z. Ge, F. Dayoub, B. Upcroft, T. Perez, and C. McCool, “Deepfruits: A fruit detection system using deep neural networks,” *sensors*, vol. 16, no. 8, p. 1222, 2016.
- [5] T.-Y. Lin, M. Maire, S. Belongie, J. Hays, P. Perona, D. Ramanan, P. Dollár, and C. L. Zitnick, “Microsoft coco: Common objects in context,” in *European conference on computer vision*. Springer, 2014.
- [6] N. Sünderhauf, F. Dayoub, D. Hall, J. Skinner, H. Zhang, G. Carneiro, and P. Corke, “A probabilistic challenge for object detection,” *Nature Machine Intelligence*, vol. 1, no. 9, pp. 443–443, 2019.
- [7] S. Zhang, Y. Xie, J. Wan, H. Xia, S. Z. Li, and G. Guo, “Widerperson: A diverse dataset for dense pedestrian detection in the wild,” *IEEE Transactions on Multimedia*, vol. 22, no. 2, pp. 380–393, 2019.
- [8] D. Miller, L. Nicholson, F. Dayoub, and N. Sünderhauf, “Dropout sampling for robust object detection in open-set conditions,” in *IEEE International Conference on Robotics and Automation*, 2018, pp. 1–7.
- [9] D. Miller, N. Sünderhauf, M. Milford, and F. Dayoub, “Uncertainty for identifying open-set errors in visual object detection,” *IEEE Robotics and Automation Letters*, vol. 7, no. 1, pp. 215–222, 2021.
- [10] “DARPA subterranean challenge,” <https://www.subtchallenge.com>, accessed: 2022-02-18.
- [11] N. Sünderhauf, O. Brock, W. Scheirer, R. Hadsell, D. Fox, J. Leitner, B. Upcroft, P. Abbeel, W. Burgard, M. Milford *et al.*, “The limits and potentials of deep learning for robotics,” *The International Journal of Robotics Research*, vol. 37, no. 4-5, pp. 405–420, 2018.
- [12] D. Bolya, S. Foley, J. Hays, and J. Hoffman, “Tide: A general toolbox for identifying object detection errors,” in *European Conference on Computer Vision*. Springer, 2020, pp. 558–573.
- [13] S. Ren, K. He, R. Girshick, and J. Sun, “Faster r-cnn: Towards real-time object detection with region proposal networks,” *arXiv preprint arXiv:1506.01497*, 2015.
- [14] T.-Y. Lin, P. Goyal, R. Girshick, K. He, and P. Dollár, “Focal loss for dense object detection,” in *Proceedings of the IEEE international conference on computer vision*, 2017, pp. 2980–2988.
- [15] Z. Cai and N. Vasconcelos, “Cascade r-cnn: Delving into high quality object detection,” in *Proceedings of the IEEE conference on computer vision and pattern recognition*, 2018, pp. 6154–6162.
- [16] J. Redmon and A. Farhadi, “Yolo9000: better, faster, stronger,” in *Proceedings of the IEEE conference on computer vision and pattern recognition*, 2017, pp. 7263–7271.
- [17] ———, “Yolov3: An incremental improvement,” *arXiv preprint arXiv:1804.02767*, 2018.
- [18] W. Liu, D. Anguelov, D. Erhan, C. Szegedy, S. Reed, C.-Y. Fu, and A. C. Berg, “Ssd: Single shot multibox detector,” in *European conference on computer vision*. Springer, 2016, pp. 21–37.
- [19] M. Everingham, L. Van Gool, C. K. Williams, J. Winn, and A. Zisserman, “The pascal visual object classes (voc) challenge,” *International journal of computer vision*, vol. 88, no. 2, pp. 303–338, 2010.
- [20] D. Hoiem, Y. Chodpathumwan, and Q. Dai, “Diagnosing error in object detectors,” in *European conference on computer vision*. Springer, 2012, pp. 340–353.
- [21] Q. M. Rahman, N. Sünderhauf, and F. Dayoub, “Did you miss the sign? a false negative alarm system for traffic sign detectors,” in *2019 IEEE/RSJ International Conference on Intelligent Robots and Systems (IROS)*. IEEE, 2019, pp. 3748–3753.
- [22] M. S. Ramanagopal, C. Anderson, R. Vasudevan, and M. Johnson-Roberson, “Failing to learn: Autonomously identifying perception failures for self-driving cars,” *IEEE Robotics and Automation Letters*, vol. 3, no. 4, pp. 3860–3867, 2018.
- [23] Q. Yang, H. Chen, Z. Chen, and J. Su, “Introspective false negative prediction for black-box object detectors in autonomous driving,” *Sensors*, vol. 21, no. 8, p. 2819, 2021.
- [24] T.-Y. Lin, P. Dollár, R. Girshick, K. He, B. Hariharan, and S. Belongie, “Feature pyramid networks for object detection,” in *Proceedings of the IEEE conference on computer vision and pattern recognition*, 2017, pp. 2117–2125.
- [25] Y. Wu, A. Kirillov, F. Massa, W.-Y. Lo, and R. Girshick, “Detectron2,” <https://github.com/facebookresearch/detectron2>, 2019.
- [26] Y. P. Loh and C. S. Chan, “Getting to know low-light images with the exclusively dark dataset,” *Computer Vision and Image Understanding*, vol. 178, pp. 30–42, 2019.
- [27] G. Pasquale, C. Ciliberto, F. Odone, L. Rosasco, and L. Natale, “Are we done with object recognition? the icub robot’s perspective,” *Robotics and Autonomous Systems*, vol. 112, pp. 260–281, 2019.
- [28] G. Metta, L. Natale, F. Nori, G. Sandini, D. Vernon, L. Fadiga, C. Von Hofsten, K. Rosander, M. Lopes, J. Santos-Victor *et al.*, “The icub humanoid robot: An open-systems platform for research in cognitive development,” *Neural networks*, vol. 23, no. 8-9, pp. 1125–1134, 2010.
- [29] N. H. et al., “Heterogeneous ground and air platforms, homogeneous sensing: Team CSIRO Data61’s approach to the darpa subterranean challenge,” 2021.
- [30] K. He, X. Zhang, S. Ren, and J. Sun, “Deep residual learning for image recognition,” in *Proceedings of the IEEE conference on computer vision and pattern recognition*, 2016, pp. 770–778.
- [31] K. Oksuz, B. C. Cam, S. Kalkan, and E. Akbas, “Imbalance problems in object detection: A review,” *IEEE transactions on pattern analysis and machine intelligence*, vol. 43, no. 10, pp. 3388–3415, 2020.